Spin-dependent transport caused by the local magnetic moments inserted in the Aharonov–Bohm rings

2007 J. Phys.: Condens. Matter 19 246207

(http://iopscience.iop.org/0953-8984/19/24/246207)

IOP PUBLISHING JOURNAL OF PHYSICS: CONDENSED MATTER

J. Phys.: Condens. Matter **19** (2007) 246207 (14pp) doi:10.1088/0953-8984/19/24/246207

Spin-dependent transport caused by the local magnetic moments inserted in the Aharonov–Bohm rings

I A Shelykh[1,2], M A Kulov[1], N G Galkin[3] and N T Bagraev[4]

[1] St Petersburg State Polytechnical University, Polytechnicheskaya 29, 195251, St Petersburg, Russia
[2] International Center for Condensed Matter Physics, Universidade de Brasilia, 70904-970 Brasili-DF, Brazil
[3] Algodign LLC, Force Field Lab, 123379, Moscow, Russia
[4] A F Ioffe Physico-Technical Institute, Polytechnicheskaya 26, 194021, St Petersburg, Russia

Received 20 March 2007, in final form 25 April 2007
Published 18 May 2007
Online at stacks.iop.org/JPhysCM/19/246207

Abstract

We analyse the conductance of an Aharonov–Bohm (AB) ring with a quantum point contact (QPC) that is inserted in one of its arms and which contains a single electron. The conductance of the device is calculated as a function of the one-dimensional (1D) carrier concentration and the value of the magnetic field perpendicular to the plane of the AB ring. The exchange interaction between the electron localized inside QPC and freely propagating electrons is shown to modify the conductance pattern at small carrier concentration significantly, giving rise to the effects related to the formation of the '0.7 feature' in the quantum conductance staircase.

1. Introduction

The recent progress in nanotechnology has allowed the preparation of quasi-one-dimensional semiconductor systems with low density of high-mobility charge carriers, which exhibit ballistic behaviour when the transport relaxation time, $\tau = m^* \mu / e$, is longer than the time of electron–electron interaction, $\hbar / k_B T$, thereby leading to the condition $k_B T \tau / \hbar > 1$. The transport of the carriers in such systems is of a coherent nature, which is revealed by the experimental findings of the quantum interference phenomena [1–15]. Since the ballistic carrier transport is not accompanied by Joule losses, the conductance of the quantum wires and the quantum point contacts (QPCs) that represent the variety of the quasi-one-dimensional semiconductor systems depends only on the number of the open channels, N, and transmission coefficient, T, at small drain–source biases [14, 15]:

$$G_0 = g_s \frac{e^2}{h} NT \tag{1}$$

where the spin factor, g_s, describes the spin degeneration of the wire's mode. The number of channels, N, can be changed by varying the split-gate voltage, V_g, which results in the

fabrication of a quantum wire connecting the two two-dimensional (2D) reservoirs [10]. Thus, the dependence G (V_g) represents the quantum conductance staircase, because the conductance of the quantum wire is changed by the value of $g_s e^2/h$ each time the Fermi level coincides with one of the 1D subbands [11, 12].

In contrast to the diffusion mode, the role of spin correlations in ballistic transport processes is considerably enhanced [2–6], specifically when only a single propagation channel is occupied. Among their most dramatic manifestations is the appearance of the '$0.7(2e^2/h)$' feature, which is split off from the first step in the quantum conductance staircase revealed by a 1D channel [1, 7–9]. Two experimental observations indicate the importance of the spin component for the behaviour of this '$0.7(2e^2/h)$' feature. Firstly, the electron g-factor was found to increase from 0.4 to 1.3 as the number of occupied 1D subbands decreases [7]. Secondly, the height of the '$0.7(2e^2/h)$' feature attains a value of '$0.5(2e^2/h)$' in a strong external magnetic field [7–9]. These results have defined the spontaneous spin polarization of a 1D gas in a zero magnetic field as one of the probable mechanisms for the '$0.7(2e^2/h)$' feature [16–18].

The model of a quantum point contact containing only one localized electron is rather promising for an explanation of the '$0.7(2e^2/h)$' feature [19–22], as containing nonzero magnetic moment this state affects the propagating carriers via exchange interaction. Since it is defined by the mutual orientation of their spins, the transmission coefficient through a QPC with a magnetic moment is spin dependent. Besides, if the triplet state energy is lower than the singlet state one, the potential barrier formed by the QPC region for the carrier in the singlet configuration is higher than for the triplet state. Therefore at small concentration of carriers the ingoing electron in the triplet configuration passes the QPC freely, while the carriers in the singlet configuration are reflected, thereby defining the principal contribution of the triplet pairs to the total conductivity. In zero magnetic fields the probability of the realization of the triplet configuration is equal to $3/4$ against $1/4$ for the singlet one, and thus the QPC conductance in the regime considered is $G = 0.75(2e^2/h)$ [21, 22]. In contrast, if the singlet configuration is energetically preferable, the conductance should be equal to $G = 0.25(2e^2/h)$ [22]. The application of the external magnetic field leads to the spin polarization of both the propagating and localized carriers, thus giving rise to a conductance value $G = 0.5(2e^2/h)$.

In the present paper, for the first time, we analyse theoretically the spin-dependent transport in a double-slit Aharonov–Bohm (AB) ring with a QPC that is inserted in one of its arms and which contains the localized electron. Recently the experimental realization of such a structure has become possible [23, 24]. Without the extra QPC inserted the conductance of a two-terminal AB ring as a function of the external magnetic field exhibits the h/e conductance oscillations provided by the AB phase shifts as well as the $h/2e$ Altshuler–Aronov–Spivak (AAS) conductance oscillations due to the round trip interference [25]. The conductance as a function of the chemical potential determined by a gate voltage, V_g, applied perpendicularly to the structure's interface exhibits periodic oscillations due to the multiple scattering of the carriers inside the ring. The presence of the localized spin in one of the arms is shown to modify the oscillation pattern significantly, and lead to the nontrivial dependence of the conductance on an external magnetic field and the 1D carrier concentration, which is controlled by varying the split gate voltage, V_g.

The paper is organized as follows. In section 2 we formulate the model that is used for theoretical description of a double-slit AB ring with a QPC inserted in one of its arms. In section 3 we analyse the conductance of a quantum wire with localized magnetic moment. This auxiliary section allows us to build the spin-dependent scattering matrix of the QPC. In section 4 we calculate the conductance of a double-slit AB ring with a QPC inserted as a function of the external magnetic field and the 1D carrier concentration. The conclusions

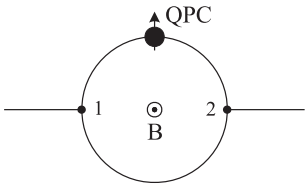

Figure 1. Schematic view of a double-slit AB ring with a QPC inserted in one of its arms.

summarize the results of the work. In the appendices we give the mathematical details of the calculations of the conductances.

2. The model

The device analysed is schematically shown in the figure 1. A double-slit AB ring is connected with symmetrically placed leads. A QPC with a single localized electron is inserted symmetrically between the ingoing and outgoing leads in one of its arms. Both the AB ring and leads are considered to be purely one-dimensional, which means that the cross section of the leads and the Fermi energy of carriers are small enough to prevent the population of the higher one-dimensional subbands, $\frac{m L^2 E_F}{\pi^2 \hbar^2} < 1$. The use of the 1D approach is a basis of the semi-analytical theory with a reasonable number of free parameters. Besides, the single-channel devices that are now achievable experimentally [23, 24, 27, 28] are preferably used comparing to the multi-channel devices because of much less effective spin relaxation [26].

In the framework of the present model we concentrate on low temperatures to provide the nearly step-liked energy distribution of the carriers in the ingoing and outgoing leads. Besides, the drain–source voltage V_{ds} is taken to be equal and small enough, $eV_{ds} \ll E_F$, so that only carriers whose energy lies in the vicinity of the Fermi surface participate in the transport. The radius of the AB ring is taken to be much smaller than inelastic scattering length to satisfy the conditions of ballistic transport. These conditions allow us to use the Landauer–Buttiker approach for the conductance calculations [14, 15].

The conjunctions between the AB ring and the leads are modelled by the QPCs which provide the elastic scattering of the carriers. The QPCs are presumed to be identical and spin independent. The latter assumption means that the spin of the carrier conserves during the passing through the QPCs. Each QPC is characterized by the amplitude of the elastic backscattering of the carrier propagating inside the lead, σ, $|\sigma| < 1$, which is determined by the system geometry. The QPCs become completely transparent if $\sigma = 0$.

An external magnetic field is applied perpendicularly to the plane of the AB ring. This field acts on both spatial and spin coordinates of the electrons moving inside the AB ring and the leads thereby define the Aharonov–Bohm phase shifts together with the Zeeman splitting. The goal of this work is to calculate the conductance of the device as a function of the external magnetic field and the concentration of electrons in the AB ring and the outgoing leads. It should be noted that the electron concentration is connected with the device Fermi energy at zero temperature or with the device chemical potential in the case of finite temperatures.

We consider the QPC dimension being much smaller than the AB ring diameter, so the propagating electrons are supposed to interact with the localized spin only in the QPC region. Thus effects similar to the formation of an electron Kondo cloud [29] in a mesoscopic one-dimensional ring are neglected. This approach is valid only for relatively high temperatures (see below).

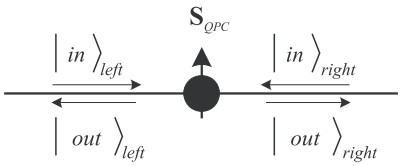

Figure 2. The scheme of the scattering in a quantum wire with a localized magnetic moment.

In the presence of an external magnetic field the propagating electrons can be characterized by their spin projection on the structure growth axis and the Fermi wavenumber. The latter is different for the two spin components due to Zeeman splitting:

$$k_{\mathrm{F}\uparrow} = \frac{\pi n_{1\mathrm{D}}}{2} + \frac{2mg_{\mathrm{e}}\mu_{\mathrm{B}}B}{\pi\hbar^2 n_{1\mathrm{D}}}, \qquad k_{\mathrm{F}\downarrow} = \frac{\pi n_{1\mathrm{D}}}{2} - \frac{2mg_{\mathrm{e}}\mu_{\mathrm{B}}B}{\pi\hbar^2 n_{1\mathrm{D}}} \tag{2}$$

where $n_{1\mathrm{D}}$ is the one-dimensional concentration of the carriers. If the external magnetic field is large enough so that

$$B > \frac{\pi^2\hbar^2 n_{1\mathrm{D}}^2}{4mg_{\mathrm{e}}\mu_{\mathrm{B}}}, \tag{3}$$

the electrons in the leads are completely polarized, and the wavenumber of the spin-up electrons is independent of the magnetic field value, $k_{F\uparrow} = \pi n_{1\mathrm{D}}$, $E_{\mathrm{F}} = \frac{\pi^2\hbar^2 n_{1\mathrm{D}}^2}{2m}$.

The interaction of the localized and propagating electrons inside the QPC can be modelled within the framework of the Heisenberg exchange Hamiltonian,

$$H_{\mathrm{int}} = V_{\mathrm{dir}} - V_{\mathrm{ex}}\boldsymbol{\sigma}_{\mathrm{e}} \cdot \boldsymbol{\sigma}_{\mathrm{S}}, \tag{4}$$

where V_{dir} characterizes the Coulomb repulsion between the electrons plus the effect of the gate applied to the QPC, V_{ex} corresponds to the exchange interaction, and the indices S and e correspond to the localized and propagating electrons, respectively.

The eigenstates of the Hamiltonian (4) correspond to the singlet and triplet states (see appendix A). In zero magnetic field the singlet and triplet state energies are split by $4V_{\mathrm{ex}}$. The position of the states depends on the sign of the coupling constant. If the 'ferromagnetic' coupling dominates, $V_{\mathrm{ex}} > 0$, the triplet configuration becomes to be preferable energetically, while the opposite case is valid for the 'antiferromagnetic' coupling, $V_{\mathrm{ex}} < 0$.

3. The conductance of a 1D quantum wire with localized magnetic moment

Before we proceed with the calculations of the conductance of an AB ring with localized magnetic moment, it is instructive to analyse the scattering in a quantum wire containing a local magnetic moment as shown in the scheme presented in figure 2. This will allow us to construct the spin-dependent scattering matrix of the QPC, which should be used in further calculations. Within the framework of our model the QPC contains a single electron interacting with freely propagating electrons by means of the Hamiltonian (4). The many-body correlations (similar to the correlations of the Kondo type [19, 20, 30]) are neglected in the present work, although we qualitatively discuss them.

Due to the exchange interaction between localized and freely propagating electrons the latter can either conserve their spin projection or undergo a spin-flip. The probabilities of these processes depend on the mutual orientation of the two spins as well as on the exchange matrix element V_{ex} (see appendix B).

If the spins of the localized and propagating electrons are parallel, only spin-conservative processes are allowed. Therefore, in this case the following 2×2 scattering matrices can be introduced:

$$\begin{pmatrix} |\uparrow\text{out}\rangle_{\text{left}} \\ |\uparrow\text{out}\rangle_{\text{right}} \end{pmatrix} = \mathbf{S}^{\uparrow\uparrow} \begin{pmatrix} |\uparrow\text{in}\rangle_{\text{left}} \\ |\uparrow\text{in}\rangle_{\text{right}} \end{pmatrix}; \qquad \begin{pmatrix} |\downarrow\text{out}\rangle_{\text{left}} \\ |\downarrow\text{out}\rangle_{\text{right}} \end{pmatrix} = \mathbf{S}^{\downarrow\downarrow} \begin{pmatrix} |\downarrow\text{in}\rangle_{\text{left}} \\ |\downarrow\text{in}\rangle_{\text{right}} \end{pmatrix} \tag{5a}$$

$$\mathbf{S}^{\uparrow\uparrow}_{\text{QPC}} = \begin{pmatrix} B_{\text{e}\uparrow,\text{S}\uparrow\to\text{e}\uparrow,\text{S}\uparrow} & A^*_{\text{e}\uparrow,\text{S}\uparrow\to\text{e}\uparrow,\text{S}\uparrow} \\ A_{\text{e}\uparrow,\text{S}\uparrow\to\text{e}\uparrow,\text{S}\uparrow} & -B^*_{\text{e}\uparrow,\text{S}\uparrow\to\text{e}\uparrow,\text{S}\uparrow} \end{pmatrix}; \qquad \mathbf{S}^{\downarrow\downarrow}_{\text{QPC}} = \begin{pmatrix} B_{\text{e}\downarrow,\text{S}\downarrow\to\text{e}\downarrow,\text{S}\downarrow} & A^*_{\text{e}\downarrow,\text{S}\downarrow\to\text{e}\downarrow,\text{S}\downarrow} \\ A_{\text{e}\downarrow,\text{S}\downarrow\to\text{e}\downarrow,\text{S}\downarrow} & -B^*_{\text{e}\downarrow,\text{S}\downarrow\to\text{e}\downarrow,\text{S}\downarrow} \end{pmatrix} \tag{5b}$$

where A and B are the amplitudes of transmission and reflection respectively, and the indices denote the spin states before and after scattering.

On the other hand, if the spins of localized and propagating electrons are antiparallel, spin-flip processes are possible and we need the 4×4 scattering matrix for the description of the interaction process. This can be recast in the following form:

$$\begin{pmatrix} |\uparrow\text{out}\rangle_{\text{left}} \\ |\uparrow\text{out}\rangle_{\text{right}} \\ |\downarrow\text{out}\rangle_{\text{left}} \\ |\downarrow\text{out}\rangle_{\text{right}} \end{pmatrix} = \mathbf{S}^{\uparrow\downarrow}_{\text{QPC}} \begin{pmatrix} |\uparrow\text{in}\rangle_{\text{left}} \\ |\uparrow\text{in}\rangle_{\text{right}} \\ |\downarrow\text{in}\rangle_{\text{left}} \\ |\downarrow\text{in}\rangle_{\text{right}} \end{pmatrix}$$

$$= \begin{pmatrix} B_{\text{e}\uparrow\text{S}\downarrow\to\text{e}\uparrow\text{S}\downarrow} & A^*_{\text{e}\uparrow\text{S}\downarrow\to\text{e}\uparrow\text{S}\downarrow} & B_{\text{e}\downarrow\text{S}\uparrow\to\text{e}\uparrow\text{S}\downarrow} & A^*_{\text{e}\downarrow\text{S}\uparrow\to\text{e}\uparrow\text{S}\downarrow} \\ A_{\text{e}\uparrow\text{S}\downarrow\to\text{e}\uparrow\text{S}\downarrow} & -B^*_{\text{e}\uparrow\text{S}\downarrow\to\text{e}\uparrow\text{S}\downarrow} & A_{\text{e}\downarrow\text{S}\uparrow\to\text{e}\uparrow\text{S}\downarrow} & -B^*_{\text{e}\downarrow\text{S}\uparrow\to\text{e}\uparrow\text{S}\downarrow} \\ B_{\text{e}\uparrow\text{S}\downarrow\to\text{e}\downarrow\text{S}\uparrow} & A^*_{\text{e}\uparrow\text{S}\downarrow\to\text{e}\downarrow\text{S}\uparrow} & B_{\text{e}\downarrow\text{S}\uparrow\to\text{e}\downarrow\text{S}\uparrow} & A^*_{\text{e}\downarrow\text{S}\uparrow\to\text{e}\downarrow\text{S}\uparrow} \\ A_{\text{e}\uparrow\text{S}\downarrow\to\text{e}\downarrow\text{S}\uparrow} & -B^*_{\text{e}\uparrow\text{S}\downarrow\to\text{e}\downarrow\text{S}\uparrow} & A_{\text{e}\downarrow\text{S}\uparrow\to\text{e}\downarrow\text{S}\uparrow} & -B^*_{\text{e}\downarrow\text{S}\uparrow\to\text{e}\downarrow\text{S}\uparrow} \end{pmatrix} \begin{pmatrix} |\uparrow\text{in}\rangle_{\text{left}} \\ |\uparrow\text{in}\rangle_{\text{right}} \\ |\downarrow\text{in}\rangle_{\text{left}} \\ |\downarrow\text{in}\rangle_{\text{right}} \end{pmatrix}. \tag{6}$$

To derive the expression for the ballistic conductance, let us consider a system of two electrons, with one localized in the QPC and one freely propagating in the ingoing lead. Before they interact, their density matrix reads

$$\begin{aligned} \boldsymbol{\rho}_{\text{in}} = \prod_k \boldsymbol{\rho}_{k,\text{in}} \otimes \boldsymbol{\rho}_{\text{s}} &= \prod_k (n_{k\uparrow}|\uparrow_{\text{e}}\rangle\langle\uparrow_{\text{e}}| + n_{k\downarrow}|\downarrow_{\text{e}}\rangle\langle\downarrow_{\text{e}}|) \otimes (P_{\text{S}\uparrow}|\uparrow_{\text{S}}\rangle\langle\uparrow_{\text{S}}| + P_{\text{S}\downarrow}|\downarrow_{\text{S}}\rangle\langle\downarrow_{\text{S}}|) \\ &= \prod_k (n_{k\uparrow}P_{\text{S}\uparrow}|\uparrow_{\text{e}}\uparrow_{\text{S}}\rangle\langle\uparrow_{\text{e}}\uparrow_{\text{S}}| + n_{k\downarrow}P_{\text{S}\downarrow}|\downarrow_{\text{e}}\downarrow_{\text{S}}\rangle\langle\downarrow_{\text{e}}\downarrow_{\text{S}}| \\ &\quad + n_{k\uparrow}P_{\text{S}\downarrow}|\uparrow_{\text{e}}\downarrow_{\text{S}}\rangle\langle\uparrow_{\text{e}}\downarrow_{\text{S}}| + n_{k\downarrow}P_{\text{S}\uparrow}|\downarrow_{\text{e}}\uparrow_{\text{S}}\rangle\langle\downarrow_{\text{e}}\uparrow_{\text{S}}|) \end{aligned} \tag{7}$$

where $n_{k\uparrow,\downarrow}$ is the mean number of electrons with definite spin projection and wavenumber, k, which is given by the Fermi distribution function,

$$n_{k\uparrow}(\mu) = \frac{1}{\text{e}^{(\hbar^2k^2/2m - g\mu_{\text{B}}B - \mu)/kT} + 1}, \qquad n_{k\downarrow}(\mu) = \frac{1}{\text{e}^{(\hbar^2k^2/2m + g\mu_{\text{B}}B - \mu)/kT} + 1}, \tag{8}$$

where μ is the chemical potential in the quantum wire. In the right lead the chemical potential is shifted down by the value eV_{ds}, and thus for the right lead μ should be substituted by $\mu - eV_{\text{ds}}$. $P_{\text{S}}\uparrow$ and $P_{\text{S}}\downarrow$ are probabilities of the localized electron findings in spin-up and spin-down states, given by the formulae

$$P_{\text{S}\uparrow} = \frac{\text{e}^{g\mu_{\text{B}}B/kT}}{\text{e}^{g\mu_{\text{B}}B/kT} + \text{e}^{-g\mu_{\text{B}}B/kT}}, \qquad P_{\text{S}\downarrow} = \frac{\text{e}^{-g\mu_{\text{B}}B/kT}}{\text{e}^{g\mu_{\text{B}}B/kT} + \text{e}^{-g\mu_{\text{B}}B/kT}}. \tag{9}$$

Using (7), the expression for the ballistic conductance of a QPC with localized magnetic moment reads

$$
\begin{aligned}
G = \frac{e\hbar}{2\pi m V_{\mathrm{ds}}} \Bigg\{ & P_{\mathrm{S}\uparrow} \int_0^\infty |A_{\mathrm{e}\uparrow\mathrm{S}\uparrow\to\mathrm{e}\uparrow\mathrm{S}\uparrow}(k)|^2 [n_{k\uparrow}(\mu) - n_{k\uparrow}(\mu - eV_{\mathrm{ds}})] k \, \mathrm{d}k \\
& + P_{\mathrm{S}\downarrow} \int_0^\infty |A_{\mathrm{e}\downarrow\mathrm{S}\downarrow\to\mathrm{e}\downarrow\mathrm{S}\downarrow}(k)|^2 [n_{k\downarrow}(\mu) - n_{k\downarrow}(\mu - eV_{\mathrm{ds}})] k \, \mathrm{d}k \\
& + P_{\mathrm{S}\downarrow} \int_0^\infty \{ |A_{\mathrm{e}\uparrow\mathrm{S}\downarrow\to\mathrm{e}\uparrow\mathrm{S}\downarrow}(k)|^2 [n_{k\uparrow}(\mu) - n_{k\uparrow}(\mu - eV_{\mathrm{ds}})] \\
& + |A_{\mathrm{e}\uparrow\mathrm{S}\downarrow\to\mathrm{e}\downarrow\mathrm{S}\uparrow}(k)|^2 [n_{k\uparrow}(\mu)(1 - n_{k\downarrow}(\mu - eV_{\mathrm{ds}})) - n_{k\uparrow}(\mu - eV_{\mathrm{ds}}) \\
& \times (1 - n_{k\downarrow}(\mu))] \} k \, \mathrm{d}k + P_{\mathrm{S}\uparrow} \int_0^\infty \{ |A_{\mathrm{e}\downarrow\mathrm{S}\uparrow\to\mathrm{e}\downarrow\mathrm{S}\uparrow}(k)|^2 [n_{k\downarrow}(\mu) - n_{k\downarrow}(\mu - eV_{\mathrm{ds}})] \\
& + |A_{\mathrm{e}\downarrow\mathrm{S}\uparrow\to\mathrm{e}\uparrow\mathrm{S}\downarrow}(k)|^2 [n_{k\downarrow}(\mu)(1 - n_{k\uparrow}(\mu - eV_{\mathrm{ds}})) - n_{k\downarrow}(\mu - eV_{\mathrm{ds}}) \\
& \times (1 - n_{k\uparrow}(\mu))] \} k \, \mathrm{d}k \Bigg\} \approx \frac{e^2\hbar}{2\pi m} \int_0^\infty \Bigg\{ [P_{\mathrm{S}\uparrow} |A_{\mathrm{e}\uparrow\mathrm{S}\uparrow\to\mathrm{e}\uparrow\mathrm{S}\uparrow}(k)|^2 \\
& + P_{\mathrm{S}\downarrow} (|A_{\mathrm{e}\uparrow\mathrm{S}\downarrow\to\mathrm{e}\uparrow\mathrm{S}\downarrow}(k)|^2 + |A_{\mathrm{e}\uparrow\mathrm{S}\downarrow\to\mathrm{e}\downarrow\mathrm{S}\uparrow}(k)|^2)] \left(\frac{\partial n_{k\uparrow}}{\partial \mu} \right) \\
& + [P_{\mathrm{S}\downarrow} |A_{\mathrm{e}\downarrow\mathrm{S}\downarrow\to\mathrm{e}\downarrow\mathrm{S}\downarrow}(k)|^2 + P_{\mathrm{S}\uparrow} (|A_{\mathrm{e}\downarrow\mathrm{S}\uparrow\to\mathrm{e}\downarrow\mathrm{S}\uparrow}(k)|^2 \\
& + |A_{\mathrm{e}\downarrow\mathrm{S}\uparrow\to\mathrm{e}\uparrow\mathrm{S}\downarrow}(k)|^2)] \left(\frac{\partial n_{k\downarrow}}{\partial \mu} \right) \\
& + [P_{\mathrm{S}\downarrow} |A_{\mathrm{e}\uparrow\mathrm{S}\downarrow\to\mathrm{e}\downarrow\mathrm{S}\uparrow}(k)|^2 - P_{\mathrm{S}\uparrow} |A_{\mathrm{e}\downarrow\mathrm{S}\uparrow\to\mathrm{e}\uparrow\mathrm{S}\downarrow}(k)|^2] \\
& \times \left[n_{k\uparrow}(\mu) \left(\frac{\partial n_{k\downarrow}}{\partial \mu} \right) - n_{k\downarrow}(\mu) \left(\frac{\partial n_{k\uparrow}}{\partial \mu} \right) \right] \Bigg\} k \, \mathrm{d}k. \qquad (10)
\end{aligned}
$$

Figure 3 shows the dependence of the single QPC conductance on the chemical potential μ for various values of temperature and external magnetic field. The parameters that have been used in the calculations are $m = 0.06\, m_{\mathrm{e}}$, $g = 2.0$, $V_{\mathrm{dir}} = 0.07\, e^2/t(4\pi\, \varepsilon_0\, L)$, $V_{\mathrm{exch}} = 0.5 V_{\mathrm{dir}}$. The length of the QPC was taken to be equal to $L = 50$ nm.

The formation of the $0.7(2e^2/h)$ feature in weak magnetic fields is predicted; it attains a value of $0.5(2e^2/h)$ in strong external magnetic fields because of the spin polarization of electrons inside the leads [7]. When the chemical potential reaches the $\mu \approx 5$ meV value, the potential barrier formed by the QPC becomes transparent for the singlet configuration, so the conductance increases to the value $2e^2/h$ (see figure 3). The oscillations seen at the $2e^2/h$ plateau are caused by the multiple scattering of the propagating electron at the edges of the QPC. In its turn, the increase of the temperature causes the strong slope of the conductance at small values of the chemical potential and reduction of the spin polarization due to the additional population of the spin-down states in the QPC and leads (see the inset in figure 3).

It should be noted that in our approach we have neglected the many-electron correlations that are similar to the Kondo-type correlations between the localized spin and propagating electrons. Their accounting for becomes crucial at extremely low temperatures, where the '0.7 feature' disappears and normal conductance quantization is recovered [20]. Within our

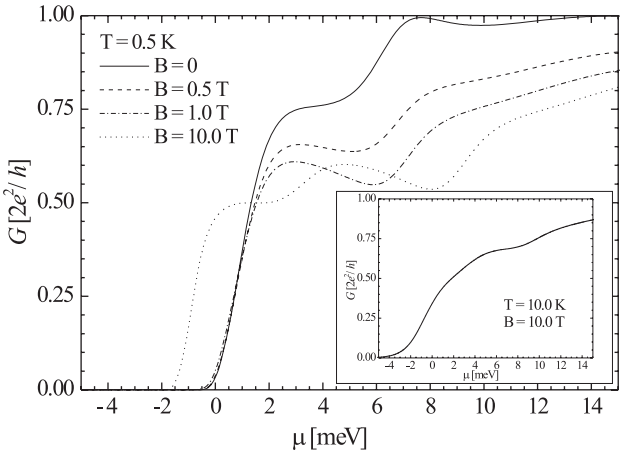

Figure 3. The conductance of a quantum wire with a QPC containing the localized electron as a function of the chemical potential at different values of the external magnetic field. $T = 0.5$ K; $B = 0$, 0.5 T, 1.0 T and 10 T. Inset: $T = 10$ K, $B = 10$ T.

model this effect can be explained using the scaling argument suggested by Anderson, who showed that accounting for correlations gives rise to the renormalization of the constant V_{ex} with temperature in the model Hamiltonian given by formula (4) [31]. In the case of antiferromagnetic interaction, the interaction constant $V_{ex} < 0$ diverges for low temperatures, leading to the formation of a Kondo cloud around the localized magnetic moment and the appearance of a pronounced Kondo minimum in the temperature dependence of the resistivity of the bulk samples. It was also argued that in quasi-1D systems accounting for the correlations of a similar type results in the nontrivial temperature dependence of the '0.7 feature', leading to its disappearance for small temperatures [19, 20]. It should be noted, however, that recent data show that the Kondo regime is not realized at least for some experimental configurations [32], and the effect is caused by the spontaneous spin-splitting of the bands [33]. This corresponds to the case of ferromagnetic interactions considered in the present paper, $V_{ex} > 0$. Qualitatively, the disappearance of the '0.7 feature' for low temperatures can be also expected in this case. Indeed, as was shown in [31] for ferromagnetic interactions, V_{ex} goes to zero with decrease of the temperature. Thus, for small temperatures the transport through a QPC becomes spin independent, and the standard value of the conductance is recovered.

Using the scattering matrices (5), (6) and the expression for the ballistic conductance (10) which takes into account all possible spin-conservative and spin-flip processes, one can proceed with the calculations of the conductance of an AB ring containing a QPC with a single localized electron.

4. The conductance of a double-slit ring that contains a QPC with localized spin

As in section 3, our consideration will be carried out within the formalism of the scattering matrix for the four possible spin orientations of the ingoing propagating and localized electrons. Therefore we should consider separately four mutual spin orientations with the corresponding amplitudes of the waves propagating inside the AB ring that are shown in figure 4.

The conductance of the ring is governed by the phase factors for the clockwise (f_1, f_3) and anticlockwise (f_1, f_3) propagating waves, which read

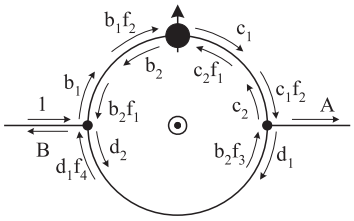

Figure 4. The amplitudes of the waves propagating in an AB ring with a QPC inserted in one of its arms.

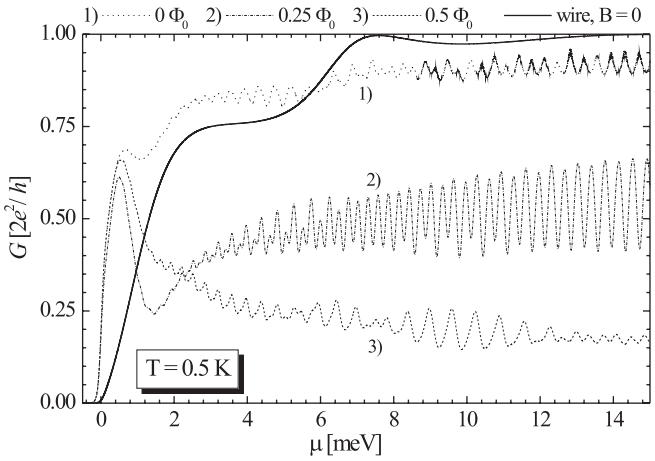

Figure 5. The conductance of a three-terminal AB ring in an external magnetic field as a function of the chemical potential. $T = 0.5$ K. 1—$\Phi = 0$, 2—$\Phi = 0.25\Phi_0$, 3—$\Phi = 0.5\Phi_0$. Solid line—the quantum wire with the localized moment at $B = 0$.

$$
\begin{aligned}
f_1 &= \exp\left[\mathrm{i}\frac{\pi}{2}\,(ka - \Phi/\Phi_0)\right] \\
f_2 &= \exp\left[\mathrm{i}\frac{\pi}{2}\,(ka + \Phi/\Phi_0)\right] \\
f_3 &= \exp\left[\mathrm{i}\pi\,(ka - \Phi/\Phi_0)\right] \\
f_4 &= \exp\left[\mathrm{i}\pi\,(ka + \Phi/\Phi_0)\right]
\end{aligned}
\tag{11}
$$

where Φ is the magnetic flux through the AB ring, Φ_0 is the elementary flux quantum, k is the wavenumber of the electron in the ring depending on its spin (if the Zeeman splitting of the bands cannot be neglected), and a is the radius of the AB ring.

The dependences of the conductance on the chemical potential and the external magnetic field can be found using scattering matrix techniques (see appendix C). They are shown in figures 5 and 6. For simplicity, we assumed that the contacts between the AB ring and the leads are completely transparent, $\sigma = 0$. The radius of the AB ring is taken as $a = 500$ nm.

Figure 5 demonstrates the dependence of the conductance on the chemical potential for different values of the flux, Φ. Oscillatory behaviour is observed, which seems to be due to interference of the triplet and singlet channels. For an AB ring of radius given above, the flux $\Phi = \Phi_0$ corresponds to an external field value equal to $B \approx 0.0026$ T. Such a magnetic field is not able to affect the transmission through a QPC with a localized electron (see figure 3). But the magnetic flux appears to control the phase of the electrons moving within an AB ring

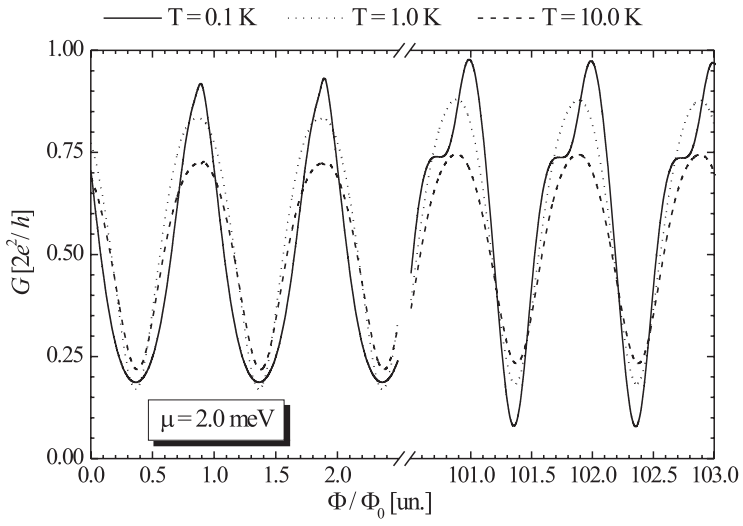

Figure 6. The conductance of a three-terminal AB ring as a function of the external magnetic field. The jump of the magnetic field was introduced to clarify the role of Zeeman splitting. $\mu = 2.0$ meV; $T = 0.1$ K, $T = 1.0$ K and $T = 10$ K.

efficiently, so that even tiny variations of the external magnetic field lead to great changes of the conductance.

In a two-terminal AB ring when the flux value is $\Phi = n\Phi_0$, where n is integer, the phase difference for electrons travelling via the upper and lower arms is equal to $2\pi n$. Thus, the conductance in this case should be exactly equal to $2e^2/h$. In contrast, when the flux is equal to a half-integer number of the flux quanta the conductance should be equal to zero. As a function of the chemical potential, the conductance of an AB ring without a QPC should demonstrate regular oscillations.

In an AB ring with a QPC containing a single electron the scattering becomes spin dependent, and thus the simple oscillatory pattern described above is drastically modified. The dependence of the conductance on the chemical potential is shown in figure 5. Two features should be mentioned here. First, although the lower arm of the ring does not contain scatterers and an ingoing electron can pass freely through it for any value of the chemical potential, the '0.7 feature' in the conductance of the upper arm is clearly reflected in the conductance of the whole system. Moreover, in zero magnetic fields, the 0.75 plateau of a single QPC seems to be split into two, as is seen from the first curve in figure 1. If an external magnetic field is applied, the plateau in the conductance is transformed into pronounced minima in the region of the small concentration, which seems to result from the interference of the singlet and triplet channels. The depth of the minima depends on the value of the magnetic field, being maximal if the number of flux quanta is half-integer (curve 3 in figure 5). Naturally, for an integer number of flux quanta the conductance is identical to the conductance for $\Phi = 0$.

The dependence of the conductance on the value of the magnetic flux is shown in figure 6. The Aharonov–Bohm phase shifts are revealed by the conductance oscillations. The asymmetry of the oscillations seems to result from spin-dependent scattering at the QPC. This asymmetry is slight for small values of the magnetic field (left part of figure 6) and becomes more pronounced in strong magnetic fields, when the effects of Zeeman splitting should be important (right part of the figure 6).

5. Conclusions

The conductance of a quantum wire with a localized magnetic moment and of an AB ring with a quantum point contact (QPC) that is inserted in one of its arms and which contains a single electron has been analysed. The conductance of both devices has been calculated as a function of the 1D carrier concentration and the external magnetic field. The exchange interaction between an electron localized inside the QPC and a freely propagating electron has been shown to modify the conductance pattern at small carrier concentrations significantly, giving rise to the effects related to the formation of the '0.7 feature' in the quantum conductance staircase. The increase of the magnetic field leads to a transformation of the '0.75 plateau' into a '0.5 plateau' due to Zeeman splitting.

The '0.7 feature' of the ballistic conductance is reflected in the conductance of the AB ring if a QPC containing a single electron is inserted in one of its arms. In zero external magnetic fields, the 0.75 plateau in the AB ring seems to be split. The application of an external magnetic field leads to the transformation of the plateau into a pronounced minimum in the region of small concentrations.

The AB oscillations of a ring containing a QPC are slightly asymmetric because of the effects of spin-dependent scattering. This asymmetry increases with the increase of the magnetic field due to the effects of Zeeman splitting.

Acknowledgments

This work has been supported by SNF in frameworks of the programme 'Scientific Cooperation between Eastern Europe and Switzerland, Grant IB7320-110970/1. IAS acknowledges support from the Brazilian Ministry of Science and Technology and from a Grant of the President of the Russian Federation.

Appendix A. Diagonalization of the exchange Hamiltonian

Let us consider the procedure of diagonalization of the Hamiltonian (4). The energy of the coupled pair of electrons within the QPC can be determined using the basis of the uncoupled states, $|\uparrow_e\uparrow_S\rangle$, $|\downarrow_e\downarrow_S\rangle$, $|\uparrow_e\downarrow_S\rangle$, $|\downarrow_e\uparrow_S\rangle$. The corresponding Hamiltonian reads

$$H = H_0 + H_{\text{Zeeman}} + H_{\text{int}} = \begin{pmatrix} \frac{\hbar^2k^2}{2m} - 2g_e\mu_B B + V_{\text{dir}} - V_{\text{ex}} & 0 & 0 & 0 \\ 0 & \frac{\hbar^2k^2}{2m} + 2g_e\mu_B B + V_{\text{dir}} - V_{\text{ex}} & 0 & 0 \\ 0 & 0 & \frac{\hbar^2k^2}{2m} + V_{\text{dir}} + V_{\text{ex}} & -2V_{\text{ex}} \\ 0 & 0 & -2V_{\text{ex}} & \frac{\hbar^2k^2}{2m} + V_{\text{dir}} + V_{\text{ex}} \end{pmatrix} \quad \text{(A.1)}$$

where the g-factors of the localized and propagating electrons are assumed to be the same. This Hamiltonian can be diagonalized by the canonical transformation

$$H' = X^{+}HX = \begin{pmatrix} \frac{\hbar^2 k^2}{2m} - 2g_e\mu_B B + V_{dir} - V_{ex} & 0 & 0 & 0 \\ 0 & \frac{\hbar^2 k^2}{2m} + 2g_e\mu_B B + V_{dir} - V_{ex} & 0 & 0 \\ 0 & 0 & \frac{\hbar^2 k^2}{2m} + V_{dir} - V_{ex} & 0 \\ 0 & 0 & 0 & \frac{\hbar^2 k^2}{2m} + V_{dir} + 3V_{ex} \end{pmatrix} \tag{A.2}$$

where the unitary operator of the transformation reads

$$X = \begin{pmatrix} 1 & 0 & 0 & 0 \\ 0 & 1 & 0 & 0 \\ 0 & 0 & 1/\sqrt{2} & -1/\sqrt{2} \\ 0 & 0 & 1/\sqrt{2} & 1/\sqrt{2} \end{pmatrix}. \tag{A.3}$$

The new eigenstates look like

$$\begin{aligned} |1\rangle &= \left|\uparrow_e\uparrow_S\right\rangle \\ |2\rangle &= \left|\downarrow_e\downarrow_S\right\rangle \\ |3\rangle &= \frac{1}{\sqrt{2}}\left(\left|\uparrow_e\downarrow_S\right\rangle + \left|\downarrow_e\uparrow_S\right\rangle\right) \\ |4\rangle &= \frac{1}{\sqrt{2}}\left(\left|\uparrow_e\downarrow_S\right\rangle - \left|\downarrow_e\uparrow_S\right\rangle\right). \end{aligned} \tag{A.4}$$

The first three of them correspond to the triplet configuration, whereas the fourth is related to the singlet configuration. In zero magnetic field the singlet and triplet state energies are split by $4V_{ex}$. The position of the states depends on the sign of the coupling constant. If the 'ferromagnetic' coupling dominates, $V_{ex} > 0$, the triplet configuration becomes preferable energetically, while the opposite case is valid for the 'antiferromagnetic' coupling, $V_{ex} < 0$.

Appendix B. Calculation of the amplitudes of spin-conservative and spin-flip processes

In this appendix we calculate the transmission and reflection amplitudes for the Hamiltonian (4).

The spin of the falling electron and the localized spin can have four mutual orientations. (1) $|1\rangle_{in} = e^{ik_\uparrow x}|\uparrow_e\uparrow_s\rangle$. This spin state is also the eigenstate of a free electron interacting with a localized electron. In the configuration considered the electron spin is conserved after passing the localized moment. Thus, the transmitted and reflected states look like

$$\begin{aligned} |1\rangle_{ref} &= B_{e\uparrow S\uparrow\to e\uparrow S\uparrow} e^{-ik_\uparrow x}\left|\uparrow_e\uparrow_s\right\rangle = r_{tr}\left(k_\uparrow\right) e^{-ik_\uparrow x}\left|\uparrow_e\uparrow_s\right\rangle \\ |1\rangle_{tr} &= A_{e\uparrow S\uparrow\to e\uparrow S\uparrow} e^{ik_\uparrow x}\left|\uparrow_e\uparrow_s\right\rangle = t_{tr}\left(k_\uparrow\right) e^{ik_\uparrow x}\left|\uparrow_e\uparrow_s\right\rangle \end{aligned} \tag{B.1}$$

where $A_{e\uparrow S\uparrow\to e\uparrow S\uparrow}$, $B_{e\uparrow S\uparrow\to e\uparrow S\uparrow}$ are the amplitudes of the transmission and the reflection in the given spin configuration, $t_{tr}(k_\uparrow)$, $r_{tr}(k_\uparrow)$ are the transmission and reflection coefficients for the carrier having the wavenumber $k_\uparrow$ falling on the barrier whose height is determined by the energy $U_{tr} = V_{dir} - V_{ex}$ corresponding to the triplet configuration of the propagating and localized electrons in the QPC. The values of $r_{tr}(k_\uparrow)$, $t_{tr}(k_\uparrow)$ can be estimated within the quasiclassical approximation if the effective length of the QPC is known.

(2) $|2\rangle_{\rm in} = {\rm e}^{{\rm i}k_\downarrow x}|\downarrow_{\rm e}\downarrow_{\rm s}\rangle$. The situation is analogous to the previous one,

$$\begin{array}{l} |2\rangle_{\rm ref} = B_{{\rm e}\downarrow{\rm S}\downarrow\to{\rm e}\downarrow{\rm S}\downarrow}{\rm e}^{-{\rm i}k_\downarrow x}\left|\downarrow_{\rm e}\downarrow_{\rm s}\right\rangle = r_{\rm tr}\left(k_\downarrow\right){\rm e}^{-{\rm i}k_\downarrow x}\left|\downarrow_{\rm e}\downarrow_{\rm s}\right\rangle \\ |2\rangle_{\rm tr} = A_{{\rm e}\downarrow{\rm S}\downarrow\to{\rm e}\downarrow{\rm S}\downarrow}{\rm e}^{{\rm i}k_\downarrow x}\left|\downarrow_{\rm e}\downarrow_{\rm s}\right\rangle = t_{\rm tr}\left(k_\downarrow\right){\rm e}^{{\rm i}k_\downarrow x}\left|\downarrow_{\rm e}\downarrow_{\rm s}\right\rangle \end{array}. \tag{B.2}$$

(3) $|3\rangle_{\rm in} = {\rm e}^{{\rm i}k_\uparrow x}|\uparrow_{\rm e}\downarrow_{\rm s}\rangle$. This case is more difficult to be analysed compared to the previous ones, because during the passing through the QPC region the propagating electron can undergo a spin-flip, and thus the state $|3\rangle$ is coupled with a state $|4\rangle_{\rm in} = {\rm e}^{{\rm i}k_\uparrow x}|\downarrow_{\rm e}\uparrow_{\rm s}\rangle$. To determine the scattering amplitudes, one should divide the QPC region into the three zones: (1) the ingoing lead, $x < 0$, (2) the region of the barrier formed by a localized spin, $0 < x < L$, and (3) outgoing lead, $x > L$. It should be noted that during the spin-flip process the energy of the localized electron is reduced by the value $2g\mu_{\rm B}B$, thus the energy of the propagating electron increases by the same value. This means that a reflected (and transmitted) electron which has undergone a spin-flip possesses the energy $E = E_{\rm F} + 2g\mu_{\rm B}B$, and although it propagates in the spin-down mode, its wavevector remains the same.

The wavefunction of electrons in zones 1 and 3 can be represented as

$$\psi_1 = \begin{pmatrix}1\\0\end{pmatrix}{\rm e}^{{\rm i}k_\uparrow x} + B_{{\rm e}\uparrow{\rm S}\downarrow\to{\rm e}\uparrow{\rm S}\downarrow}\begin{pmatrix}1\\0\end{pmatrix}{\rm e}^{-{\rm i}k_\uparrow x} + B_{{\rm e}\uparrow{\rm S}\downarrow\to{\rm e}\downarrow{\rm S}\uparrow}\begin{pmatrix}0\\1\end{pmatrix}{\rm e}^{-{\rm i}k_\uparrow x} \tag{B.3a}$$

$$\psi_3 = A_{{\rm e}\uparrow{\rm S}\downarrow\to{\rm e}\uparrow{\rm S}\downarrow}\begin{pmatrix}1\\0\end{pmatrix}{\rm e}^{{\rm i}k_\uparrow x} + A_{{\rm e}\uparrow{\rm S}\downarrow\to{\rm e}\downarrow{\rm S}\uparrow}\begin{pmatrix}0\\1\end{pmatrix}{\rm e}^{{\rm i}k_\uparrow x}. \tag{B.3b}$$

Finally, the wavefunction in the intermediate region should be determined. Using the formula (A.2), one easily obtains

$$\psi_2 = C\begin{pmatrix}1\\1\end{pmatrix}{\rm e}^{{\rm i}k_1 x} + D\begin{pmatrix}1\\1\end{pmatrix}{\rm e}^{-{\rm i}k_1 x} + G\begin{pmatrix}1\\-1\end{pmatrix}{\rm e}^{{\rm i}k_2 x} + F\begin{pmatrix}1\\-1\end{pmatrix}{\rm e}^{-{\rm i}k_2 x} \tag{B.4}$$

where

$$k_1 = \sqrt{\frac{2m}{\hbar^2}\left(E_{\rm F} + g\mu_{\rm B}B - V_{\rm dir} + V_{\rm ex}\right)} \tag{B.5a}$$

$$k_2 = \sqrt{\frac{2m}{\hbar^2}\left(E_{\rm F} + g\mu_{\rm B}B - V_{\rm dir} - 3V_{\rm ex}\right)}. \tag{B.5b}$$

The upper value corresponds to the triplet configuration of the propagating and localized electron, whereas the lower value is related to the singlet configuration. Thus, the complete wavefunction contains eight unknown constants: $A_{{\rm e}\uparrow{\rm S}\downarrow\to{\rm e}\uparrow{\rm S}\downarrow}$, $A_{{\rm e}\uparrow{\rm S}\downarrow\to{\rm e}\downarrow{\rm S}\uparrow}$, $B_{{\rm e}\uparrow{\rm S}\downarrow\to{\rm e}\uparrow{\rm S}\downarrow}$, $B_{{\rm e}\uparrow{\rm S}\downarrow\to{\rm e}\downarrow{\rm S}\uparrow}$, C, D, F, G. They can be easily found from the system of the linear equations obtained by matching the wavefunctions and their derivatives at the points $x = 0$ and $x = L$.

(4) $|4\rangle_{\rm in} = {\rm e}^{{\rm i}k_\downarrow x}|\downarrow_{\rm e}\uparrow_{\rm s}\rangle$. The procedure is analogous to one described above. The wavefunction now looks like

$$\psi_1 = \begin{pmatrix}0\\1\end{pmatrix}{\rm e}^{{\rm i}k_\downarrow x} + B_{{\rm e}\downarrow{\rm S}\uparrow\to{\rm e}\downarrow{\rm S}\uparrow}\begin{pmatrix}0\\1\end{pmatrix}{\rm e}^{-{\rm i}k_\downarrow x} + B_{{\rm e}\downarrow{\rm S}\uparrow\to{\rm e}\uparrow{\rm S}\downarrow}\begin{pmatrix}1\\0\end{pmatrix}{\rm e}^{-{\rm i}k_\downarrow x} \tag{B.6a}$$

$$\psi_3 = A_{{\rm e}\downarrow{\rm S}\uparrow\to{\rm e}\downarrow{\rm S}\uparrow}\begin{pmatrix}0\\1\end{pmatrix}{\rm e}^{{\rm i}k_\downarrow x} + A_{{\rm e}\downarrow{\rm S}\uparrow\to{\rm e}\uparrow{\rm S}\downarrow}\begin{pmatrix}0\\1\end{pmatrix}{\rm e}^{{\rm i}k_\downarrow x} \tag{B.6b}$$

$$\psi_2 = C\begin{pmatrix}1\\1\end{pmatrix}{\rm e}^{{\rm i}k_1 x} + D\begin{pmatrix}1\\1\end{pmatrix}{\rm e}^{-{\rm i}k_1 x} + G\begin{pmatrix}1\\-1\end{pmatrix}{\rm e}^{{\rm i}k_2 x} + F\begin{pmatrix}1\\-1\end{pmatrix}{\rm e}^{-{\rm i}k_2 x}. \tag{B.6c}$$

Again, the coefficients are determined from the continuity conditions at $x = 0$ and $x = L$.

Appendix C. Calculation of the scattering amplitudes of a ring with embedded QPC

If the spins of the localized and freely propagating electrons are parallel, the unknown amplitudes of the waves propagating in the ring (shown in figure 4) are connected by the following set of the linear equations:

$$\begin{pmatrix} b_1 \\ B \\ d_2 \end{pmatrix} = \mathbf{S}_{\text{conj}} \begin{pmatrix} b_2 f_1 \\ 1 \\ d_1 f_4 \end{pmatrix} = \begin{pmatrix} r & \varepsilon & t \\ \varepsilon & \sigma & \varepsilon \\ t & \varepsilon & r \end{pmatrix} \begin{pmatrix} b_2 f_1 \\ 1 \\ d_1 f_4 \end{pmatrix} \tag{C.1a}$$

$$\begin{pmatrix} c_2 \\ A \\ d_1 \end{pmatrix} = \mathbf{S}_{\text{conj}} \begin{pmatrix} c_1 f_2 \\ 0 \\ d_2 f_3 \end{pmatrix} = \begin{pmatrix} r & \varepsilon & t \\ \varepsilon & \sigma & \varepsilon \\ t & \varepsilon & r \end{pmatrix} \begin{pmatrix} c_1 f_2 \\ 0 \\ d_2 f_3 \end{pmatrix} \tag{C.1b}$$

$$\begin{pmatrix} c_1 \\ b_2 \end{pmatrix} = \begin{pmatrix} r_{\text{tr,QPC}} & t^*_{\text{tr,QPC}} \\ t_{\text{tr,QPC}} & -r^*_{\text{tr,QPC}} \end{pmatrix} \begin{pmatrix} c_2 f_1 \\ b_1 f_2 \end{pmatrix} \tag{C.1c}$$

where we introduced the scattering matrix of the conjunction of the leads and the AB ring, $\mathbf{S}_{\text{conj}}$. The conditions of unitarity give the equations connecting $r, t, \varepsilon, \sigma$ coefficients (see [34, 35]). These equations allow the determination of the transmission amplitudes through the system $A_{\text{e}\uparrow\text{S}\uparrow\to\text{e}\uparrow\text{S}\uparrow}(k)$ and $A_{\text{e}\downarrow\text{S}\downarrow\to\text{e}\downarrow\text{S}\downarrow}(k)$.

The case of the anti-parallel orientation of spins of the localized and falling electron is more difficult to be analysed. All amplitudes in figure 4 are now spinors, e.g. $\mathbf{b}_1 = (b_{1\uparrow}, b_{1\downarrow})^+$. Consequently, the phase factors are diagonal 2×2 matrices. If the contacts between the AB ring and the leads are spin-conservative, the equation for the amplitudes reads, in block form,

$$\begin{pmatrix} b_{1\uparrow} \\ B_{\text{e}\uparrow\text{S}\downarrow\to\text{e}\uparrow\text{S}\downarrow} \\ d_{2\uparrow} \\ b_{1\downarrow} \\ B_{\text{e}\uparrow\text{S}\downarrow\to\text{e}\downarrow\text{S}\uparrow} \\ d_{2\downarrow} \end{pmatrix} = \begin{pmatrix} \mathbf{S}_{\text{conj}} & 0 \\ 0 & \mathbf{S}_{\text{conj}} \end{pmatrix} \begin{pmatrix} b_{2\uparrow} f_{1\uparrow} \\ 1 \\ d_{1\uparrow} f_{4\uparrow} \\ b_{2\downarrow} f_{1\downarrow} \\ 0 \\ d_{1\downarrow} f_{4\downarrow} \end{pmatrix} \tag{C.2a}$$

$$\begin{pmatrix} c_{2\uparrow} \\ A_{\text{e}\uparrow\text{S}\downarrow\to\text{e}\uparrow\text{S}\downarrow} \\ d_{1\uparrow} \\ c_{2\downarrow} \\ A_{\text{e}\uparrow\text{S}\downarrow\to\text{e}\downarrow\text{S}\uparrow} \\ d_{1\downarrow} \end{pmatrix} = \begin{pmatrix} \mathbf{S}_{\text{conj}} & 0 \\ 0 & \mathbf{S}_{\text{conj}} \end{pmatrix} \begin{pmatrix} c_{1\uparrow} f_{2\uparrow} \\ 1 \\ d_{2\uparrow} f_{3\uparrow} \\ c_{1\downarrow} f_{2\downarrow} \\ 0 \\ d_{2\downarrow} f_{3\downarrow} \end{pmatrix} \tag{C.2b}$$

$$\begin{pmatrix} c_{1\uparrow} \\ b_{2\uparrow} \\ c_{1\downarrow} \\ b_{2\downarrow} \end{pmatrix} = \mathbf{S}^{\uparrow\downarrow}_{\text{QPC}} \begin{pmatrix} c_{2\uparrow} f_{1\uparrow} \\ b_{1\uparrow} f_{2\uparrow} \\ c_{2\downarrow} f_{1\downarrow} \\ b_{1\downarrow} f_{2\downarrow} \end{pmatrix}. \tag{C.2c}$$

Here we assumed that the falling electron is in the spin-up state and the localized electron in the spin-down state. If the opposite situation is realized, in (C.2*a*) the column in the right-hand side should be changed as follows:

$$\begin{pmatrix} b_{2\uparrow} f_{1\uparrow} \\ 1 \\ d_{1\uparrow} f_{4\uparrow} \\ b_{2\downarrow} f_{1\downarrow} \\ 0 \\ d_{1\downarrow} f_{4\downarrow} \end{pmatrix} \Rightarrow \begin{pmatrix} b_{2\uparrow} f_{1\uparrow} \\ 0 \\ d_{1\uparrow} f_{4\uparrow} \\ b_{2\downarrow} f_{1\downarrow} \\ 1 \\ d_{1\downarrow} f_{4\downarrow} \end{pmatrix}. \tag{C.3}$$

Solving the system of the equations (C.2) and (C.3), the transmission amplitudes for the ingoing spin-up and spin-down electrons with and without spin-flip, $A_{\text{e}\uparrow\text{S}\downarrow\to\text{e}\uparrow\text{S}\downarrow}$, $A_{\text{e}\uparrow\text{S}\downarrow\to\text{e}\downarrow\text{S}\uparrow}$,

$A_{e\downarrow S\uparrow\to e\uparrow S\downarrow}$, $A_{e\downarrow S\uparrow\to e\downarrow S\uparrow}$, can be obtained, which allow the calculation of the conductance by means of equation (10).

References

[1] Pyshkin K S, Ford C J B, Harrell R H, Pepper M, Linfield E H and Ritchie D A 2000 *Phys. Rev.* B **62** 15842
[2] Pudalov V M 1998 *Phys.—Usp.* **41** 211
[3] Finkel'stein A M 1983 *Sov. Phys.—JETP* **57** 97
[4] Zala G, Narozhny B N and Aleiner I L 2001 *Phys. Rev.* B **64** 201201(R)
[5] Rashba E I 2002 *J. Supercond.* **15** 1
[6] Fukuyama H, Platzman P M and Anderson P W 1979 *Phys. Rev.* B **19** 5211
[7] Thomas K J, Nicholls J T, Simmons M Y, Pepper M, Mace D R and Ritchie D A 1996 *Phys. Rev. Lett.* **77** 135
[8] Thomas K J, Nicholls J T, Appleyard N J, Simmons M Y, Pepper M, Mace D R, Tribe W R and Ritchie D A 1998 *Phys. Rev.* B **58** 4846
[9] Thomas K J, Nicholls J T, Pepper M, Tribe W R, Simmons M Y and Ritchie D A 2000 *Phys. Rev.* B **61** R13365
[10] Thornton T J, Pepper M, Ahmed H, Andrews D and Davies G J 1986 *Phys. Rev. Lett.* **56** 1198
[11] Wharam D A, Thornton T J, Newbury R, Pepper M, Ahmed H, Frost J E F, Hasko E G, Peacock E C, Ritchie D A and Jones G A C 1988 *J. Phys. C: Solid State Phys.* **21** L209
[12] van Wees B J, van Houten H, Beenakker C W J, Williamson J G, Kouwenhoven L P, van der Marel D and Foxon C T 1988 *Phys. Rev. Lett.* **60** 848
[13] Yacoby A, Stormer H L, Wingreen N S, Pfeiffer L N, Baldwin K W and West K W 1996 *Phys. Rev. Lett.* **77** 4612
[14] Landauer R 1957 *IBM J. Res. Dev.* **1** 233
[15] Buttiker M 1986 *Phys. Rev. Lett.* **57** 1761
[16] Wang C-K and Berggren K-F 1998 *Phys. Rev.* B **57** 4552
[17] Starikov A A, Yakimenko I I and Berggren K-F 2003 *Phys. Rev.* B **67** 235319
[18] Bagraev N T, Shelykh I A, Ivanov V K and Klyachkin L E 2004 *Phys. Rev.* B **70** 155315
[19] Meir Y, Hirose K and Wingreen N S 2002 *Phys. Rev. Lett.* **89** 196802
[20] Cronenwett S M, Lynch H J, Goldhaber-Gordon D, Kouwenhoven L P, Marcus C M, Hirose K, Wingreen N S and Umansky V 2002 *Phys. Rev. Lett.* **88** 226805
[21] Flambaum V V and Kuchiev M Yu 2000 *Phys. Rev.* B **61** R7869
[22] Rejec T, Ramsak A and Jefferson J H 2003 *Phys. Rev.* B **67** 075311
[23] Bagraev N T, Buralev A D, Gehlhoff W, Ivanov V K, Klyachkin L E and Shelykh I A 2002 *Semiconductors* **36** 462
[24] Bagraev N T, Galkin N G, Gehlhoff W, Klyachkin L E, Malyarenko A M and Shelykh I A 2006 *J. Phys.: Condens. Matter* **18** L567
[25] Altshuler B L, Aronov A G and Spivak B Z 1981 *Sov. Phys.—JETP Lett.* **33** 94
[26] Pramanik S, Bandyophay S and Cahay M 2004 *Preprint* cond-mat/0403021
[27] Schuster R, Buks E, Heiblum M, Mahalu D, Umansky V and Shtrikman H 1997 *Nature* **385** 417
[28] Bagraev N T, Bouravleuv A D, Gehlhoff W, Ivanov V K, Klyachkin L E, Malyarenko A M, Rykov S A and Shelykh I A 2002 *Physica* E **12** 762
[29] Affleck I and Simon P 2001 *Phys. Rev. Lett.* **86** 2854
[30] Rejec T and Meir Y 2006 *Nature* **442** 900
[31] Anderson P W 1970 *J. Phys. C: Solid State Phys.* **3** 2436
[32] Graham A C, Sawkey D L, Pepper M, Simmons M Y and Ritchie D A 2007 *Phys. Rev.* B **75** 035331
[33] Graham A C, Thomas K J, Pepper M, Cooper N R, Simmons M Y and Ritchie D A 2003 *Phys. Rev. Lett.* **91** 136404
[34] Buttiker M, Ymry Y and Azbel M Ya 1984 *Phys. Rev.* A **30** 1982
[35] Shelykh I A, Bagraev N T, Galkin N G and Klyachkin L E 2005 *Phys. Rev.* B **71** 113311